Thermodynamic Studies of Rod- and Spindle-Shaped β-FeOOH Crystals

Chengzhen Wei,† Xiaoming Wang,† Zhaodong Nan,*,† and Zhicheng Tan‡

College of Chemistry and Chemical Engineering, Yangzhou University, Yangzhou 225002, China, and Thermochemistry Laboratory, Dalian Institute of Chemical Physics, Chinese Academy of Sciences, Dalian 116023, China

Different morphologies of β-FeOOH including rod- and spindle-shaped crystals were synthesized via a hydrothermal reaction at low temperature. The molar heat capacities of the obtained samples were determined by a precision automated adiabatic calorimeter over the temperature range of (78 to 390) K. The observed results demonstrated that the change of the molar heat capacity with thermodynamic temperature was different for the rod and spindle-shaped β-FeOOH crystals. Polynomial equations of the molar heat capacities as a function of temperature were fitted by a least-squares method for the rod- and spindle-shaped β-FeOOH crystals. Smoothed heat capacities and thermodynamic functions of the obtained samples, such as $H(T/K) - H(298.15)$ and $S(T/K) - S(298.15)$, were calculated on the basis of the fitted polynomials and the relationships of the thermodynamic functions. In addition, the as-prepared samples were also characterized by X-ray powder diffraction (XRD), transmission electron microscopy (TEM), and thermal gravimetric analysis (TGA).

Introduction

In recent years, iron oxyhydroxides and iron oxides have attracted much attention owing to their excellent physical and chemical properties and potential applications in various fields, such as for use as pigments, catalysts, gas sensors, and magnetic recording media.[1−6] The polymorphs of iron oxyhydroxide consist of α-FeOOH (goethite), β-FeOOH (akaganeite), and γ-FeOOH (lepidocrocite).[7] Among the iron oxyhydroxides, β-FeOOH, as a stable iron oxide, which has a large tunnel-type structure, has received wide attention because of its unique properties. As a promising candidate for an electrode material, β-FeOOH exhibits good electrochemical properties with a high theoretical discharge capacity (302 $mA \cdot h \cdot g^{-1}$).[2] β-FeOOH has been used as a precursor for the preparation of ferromagnetic α-Fe_2O_3.[8,9] However, to the best of our knowledge, the molar heat capacities of β-FeOOH have not been reported so far. It is of great significance to obtain the molar heat capacities of β-FeOOH and furthermore to fully understand this material.

In the present paper, rod- and spindle-shaped β-FeOOH crystals were synthesized, and their molar heat capacities were measured over the temperature range of (78 to 390) K.

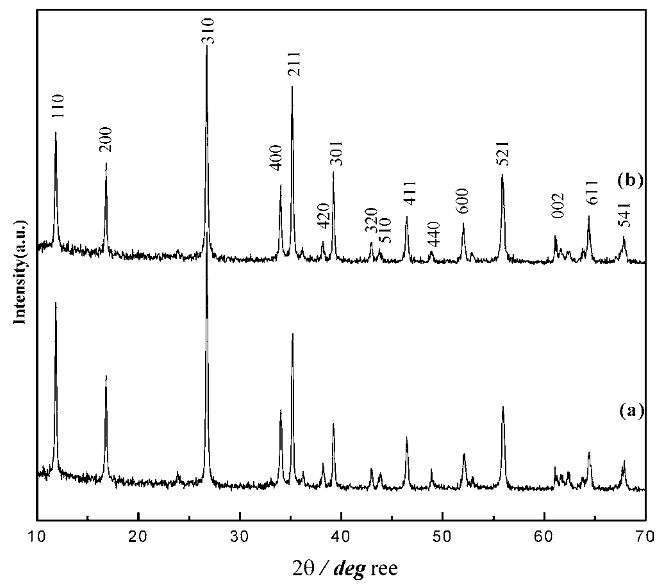

Figure 1. XRD patterns of the as-prepared β-FeOOH products, (a) rod- and (b) spindle-shaped particles.

Experimental Section

All the reagents used in this work were of analytical grade and used without further purification.

β-FeOOH nanorod particles were prepared following the procedure reported in a previous paper.[10] In a typical synthesis procedure of the β-FeOOH nanorods, $FeCl_3 \cdot 6H_2O$ (1.0134 g) and $(NH_2)_2CO$ (0.6000 g) were dissolved in distilled water (10 mL) with constant stirring over 10 min. The solution was then transferred to a flask and maintained at (90 to 95) °C under reflux for a period of 12 h, resulting in the formation of a yellow precipitate. This precipitate was collected and rinsed repeatedly with distilled water. Spindle-shaped β-FeOOH was synthesized through a facile hydrothermal route. In a typical experiment, $FeCl_3 \cdot 6H_2O$ (1.6218 g) was dissolved in 50 mL of distilled water with stirred vigorously for 10 min to form a homogeneous solution. The solution was then transferred into a flask and maintained at 90 °C under reflux for 12 h. After the reaction was completed, the resulting yellow solid precipitate was collected by centrifugation, washed several times with distilled water, and finally dried in air at 30 °C for 24 h.

The crystal phase of the as-prepared particles were identified by a Rigaku D/MAX-XA powder X-ray diffractometer with Cu Kα radiation ($\lambda = 1.5405$ Å). A scanning rate of 0.1 $deg \cdot s^{-1}$ was used to record the pattern in the 2θ range of (10 to 70) deg.

* Corresponding author. Tel.: +86-514-87959896. Fax: +86-514-87959896. E-mail: zdnan@yzu.edu.cn.
† Yangzhou University.
‡ Chinese Academy of Sciences.

10.1021/je900373z CCC: $40.75
Published on Web 09/16/2009

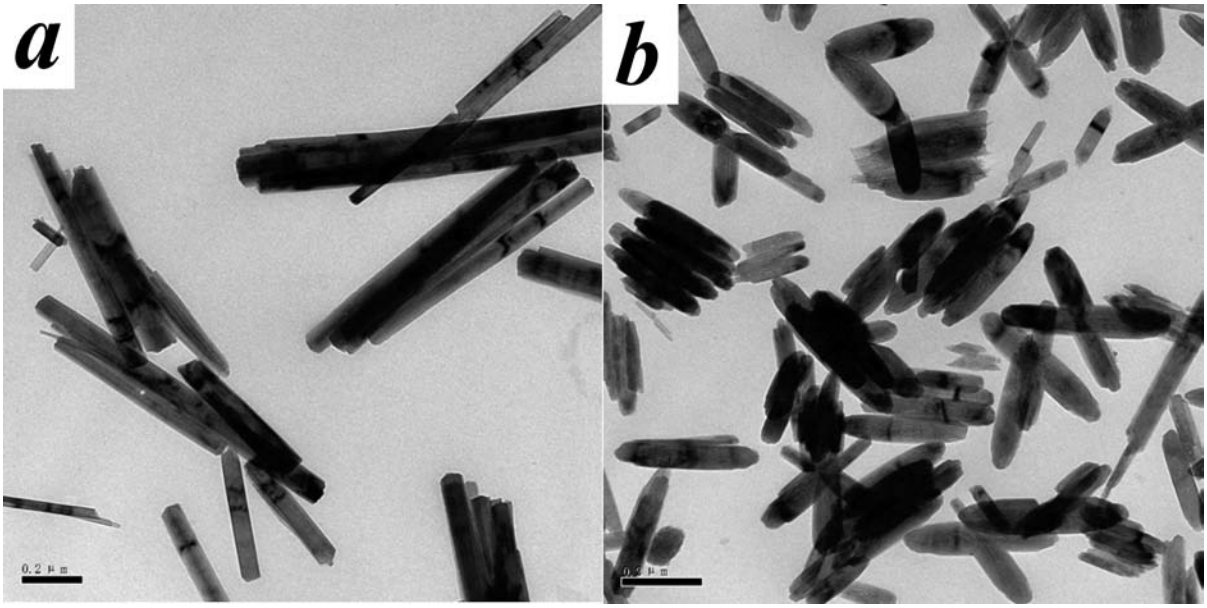

Figure 2. TEM images of the as-prepared β-FeOOH particles, (a) rod-like and (b) spindle-like (the bar = 200 nm).

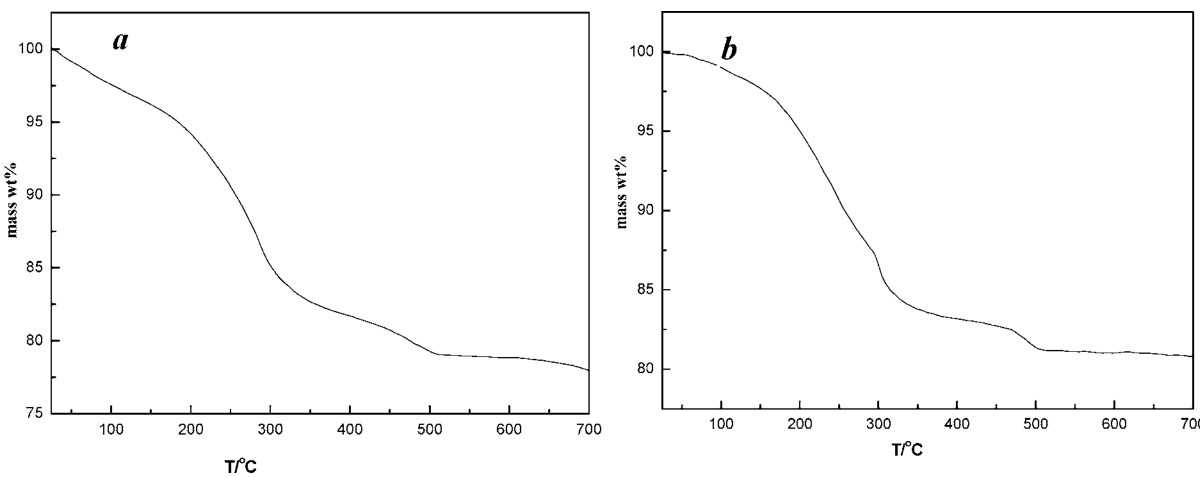

Figure 3. TGA curves of the as-prepared β-FeOOH particles, (a) spindle shape and (b) rod shape.

The morphologies and mean sizes of the obtained particles were examined by a transmission electron microscope (TEM, Hitachi, model H-800) using an accelerating voltage of 200 kV.

Thermal gravimetric analysis (TGA) of the as-obtained β-FeOOH was carried out by a thermogravimetric analysis system (model: TG 209 F1, NETZSCH, Germany). The as-prepared samples were heated from room temperature to 700 °C under nitrogen at a heating rate of 10 $°C \cdot min^{-1}$. The flow rate of nitrogen for each of the TGA experiments was controlled at 70 $mL \cdot min^{-1}$. The amounts of the samples used for TGA analysis were (18.2 and 18.8) mg for the rod- and spindle-shaped β-FeOOH crystals, respectively.

A high precision automatic adiabatic calorimeter was used to determine the heat capacities of the as-prepared products over the temperature range of (78 to 390) K. The calorimeter was established in the Thermochemistry Laboratory of the Dalian Institute of Chemical Physics, Chinese Academy of Sciences. The principle and structure of the adiabatic calorimeter have been described in detail elsewhere.[11−13] The temperature increment was controlled at (2 to 4) K during the whole experimental process.

Before determination of the heat capacity of the as-obtained samples, the reliability of the automatic adiabatic calorimeter was verified via measurements on a α-Al_2O_3 reference standard material. On the basis of our experimental results, the deviations were within ± 0.2 % compared with the values recommended by the National Bureau of Standards[14] in the temperature range of (80 to 400) K.

The mass of the rod and spindle-shaped β-FeOOH crystals used for the heat capacity determination were (1.07576 and 1.03306) g, respectively, which is equivalent to (0.0121074 and 0.0116268) mol, on the basis of the molar mass of β-FeOOH, $M = 88.8517\ g \cdot mol^{-1}$.

Results and Discussion

The composition and crystalline phase purity of the as-prepared products were examined by a powder X-ray diffraction (XRD) technique. As shown in Figure 1, all of the diffraction peaks can be indexed to a tetragonal β-FeOOH phase, which agrees well with the reported data (β-FeOOH, JCPDS no. 34-1266). No obvious XRD peaks due to impurities were found in the XRD patterns. The strong and sharp diffraction peaks can also demonstrate good crystallization of the as-prepared rod- and spindle-shaped β-FeOOH crystals.

The morphologies and mean sizes of the as-prepared β-FeOOH particles were investigated by TEM. Figure 2a,b shows the

Table 1. Experimental Molar Heat Capacity Data of the As-Prepared β-FeOOH

T	$C_{p,m}$ [a]	T	$C_{p,m}$ [a]	T	$C_{p,m}$ [b]	T	$C_{p,m}$ [b]
K	$J \cdot K^{-1} \cdot mol^{-1}$	K	$J \cdot K^{-1} \cdot mol^{-1}$	K	$J \cdot K^{-1} \cdot mol^{-1}$	K	$J \cdot K^{-1} \cdot mol^{-1}$
78.47	7.071	247.38	65.152	78.23	8.502	241.26	63.047
81.05	8.485	250.44	65.556	81.05	9.680	245.03	63.973
84.58	9.697	253.50	66.481	84.58	11.111	248.56	64.815
87.41	11.313	256.32	67.130	87.41	12.542	251.38	65.488
90.46	12.626	259.38	68.333	90.23	13.805	254.44	66.330
93.52	13.737	262.20	69.074	93.05	15.152	257.26	66.835
96.35	14.949	265.26	69.722	95.88	16.246	260.32	67.677
99.40	16.364	268.08	70.648	98.70	17.593	263.14	68.182
103.40	17.778	271.14	71.296	102.70	18.855	266.20	68.687
107.47	18.939	273.96	72.315	106.70	20.455	269.02	69.360
110.48	19.949	276.79	73.056	109.52	21.717	272.08	70.202
113.24	21.044	279.85	73.611	112.48	22.869	274.91	70.875
116.25	22.391	282.67	74.537	115.37	24.014	277.73	71.633
119.51	23.569	285.73	75.314	118.29	25.068	280.79	72.222
122.52	24.495	288.79	75.751	121.22	26.085	283.61	72.811
125.28	25.926	291.84	76.570	124.11	27.441	286.43	73.401
128.29	26.852	294.90	77.171	127.16	28.788	289.49	73.990
131.30	27.862	297.96	78.384	129.99	29.545	292.55	74.663
134.57	29.209	301.02	79.091	133.05	30.556	295.61	75.084
137.58	30.471	304.08	79.697	135.87	31.481	298.90	75.926
140.59	31.566	307.14	80.606	138.69	32.239	301.96	76.515
143.60	32.323	310.19	81.414	141.52	33.502	305.02	76.852
146.69	33.535	313.25	82.020	144.57	34.596	308.08	77.441
149.62	34.848	316.31	82.424	147.40	35.859	311.37	78.283
153.64	35.943	319.37	83.131	150.22	36.785	314.43	78.704
157.40	36.953	322.43	84.141	153.98	37.963	317.49	79.040
160.41	38.468	325.49	85.051	157.75	38.973	320.55	79.798
163.43	39.646	328.54	85.455	160.57	39.731	323.84	80.303
166.44	40.741	331.60	86.566	163.63	41.077	326.66	80.640
169.45	41.582	334.66	87.273	166.45	41.835	328.07	80.892
172.46	42.508	337.72	87.980	169.28	42.761	330.19	81.061
175.72	43.771	340.54	88.485	172.33	43.603	332.31	81.650
178.73	44.781	343.60	88.990	175.16	44.613	334.90	82.155
181.74	45.707	346.66	89.697	178.22	45.202	337.48	82.576
184.76	46.465	349.72	89.798	181.27	46.128	340.07	82.912
187.77	47.727	350.42	90.202	184.10	46.970	342.66	83.502
191.03	48.737	352.78	91.010	187.15	47.980	345.25	84.091
194.04	49.495	355.36	91.616	189.98	48.737	348.07	84.428
197.05	50.505	357.95	92.020	192.80	49.663	350.66	85.185
199.81	51.347	360.77	92.626	195.86	50.505	353.25	85.606
203.58	52.609	363.13	93.333	198.68	51.431	356.07	86.111
207.34	53.620	365.95	93.838	202.21	52.609	358.66	86.364
210.35	54.630	368.54	94.646	205.98	53.620	361.25	86.953
213.61	55.219	371.13	94.949	208.80	54.545	364.07	87.205
216.37	56.229	373.95	95.354	211.86	55.303	366.66	87.626
219.39	57.323	376.77	96.263	214.68	56.061	369.24	88.300
222.40	57.997	379.60	96.869	217.74	57.155	371.83	88.721
225.16	58.838	382.18	97.778	220.56	58.081	374.65	89.057
228.17	59.764	384.77	97.980	223.38	58.754	377.24	89.310
231.18	60.606	387.36	98.485	226.44	59.343	379.83	89.731
234.19	61.448	389.95	98.990	229.27	60.438	382.42	90.404
237.20	62.374			232.32	61.027	385.24	90.657
240.21	63.384			235.38	61.869	387.83	91.162
243.85	64.343			238.44	62.710	390.42	91.498

[a] Rod-like β-FeOOH. [b] Spindle-like β-FeOOH.

representative TEM micrographs of the as-prepared rod and spindle-shaped β-FeOOH, respectively. A typical TEM image (Figure 2a) clearly shows that the rod-like β-FeOOH has a smooth surface with an average diameter of 71 nm and an average length of 909 nm. From the TEM image of the spindle-shaped β-FeOOH (Figure 2b), a spindle shape with an average width of 94 nm and a length of 428 nm was observed.

The TGA curves of the as-prepared samples are shown in Figure 3. It is obvious that there are two mass loss steps in the temperature ranges (25 to 200 and 200 to 520) °C in Figure 3a,b, respectively. At 520 °C, the mass of the as-prepared samples no longer changes, even though heating was continued to 700 °C, which indicates that the stable residue can reasonably be ascribed to α-Fe_2O_3.[2]

The experimental molar heat capacities of the as-prepared rod- and spindle-like β-FeOOH were determined by a high precision automatic adiabatic calorimeter over the temperature range of (78 to 390) K. All of the experimental results are listed in Table 1 and shown in Figure 4. The molar heat capacities of the obtained samples are fitted to the following polynomial equations in reduced temperature (X) via least-squares fitting.

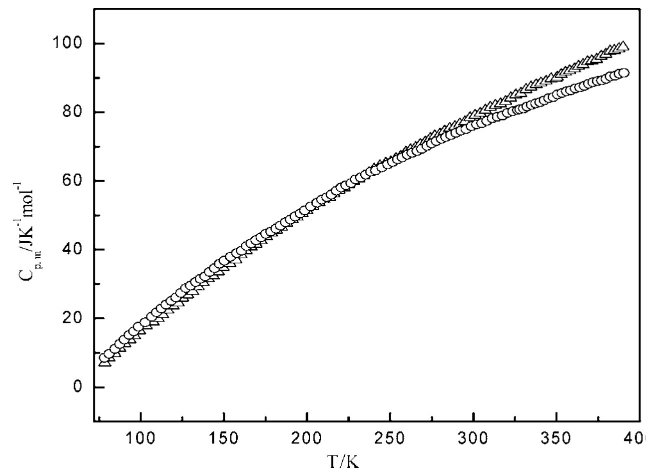

Figure 4. Experimental molar heat capacities of the as-prepared β-FeOOH against experimental temperature. Δ, rod-like; ○, spindle-shaped β-FeOOH.

For the rod-like β-FeOOH:

$$C_{p,m}/\text{J} \cdot \text{K}^{-1} \cdot \text{mol}^{-1} = 61.46 + 44.19X - 8.56X^2 + 1.66X^3 + 0.34X^4 \quad (1)$$

where X is the reduced temperature, $X = [T - (T_1 + T_2)/2]/[T_2 - T_1]/2]$, where T is the experimental temperature. In the temperature range of (78 to 390) K, $X = [(T/\text{K}) - 234.21]/155.74$, where $T_1 = 78.47$ K and $T_2 = 389.95$ K. The coefficient of determination of the fitting is $R^2 = 0.9999$, and the fitness standard error is $\delta = 0.201\ \text{J} \cdot \text{K}^{-1} \cdot \text{mol}^{-1}$. The standard δ of the fitness was calculated by the following equation:

$$\delta = \sqrt{\frac{\sum (C_{p,m}^{\text{fit}} - C_{p,m}^{\text{exp}})^2}{n - 1}} \quad (2)$$

In the equation, n is the number of the experimental points, and $C_{p,m}^{\text{exp}}$ and $C_{p,m}^{\text{fit}}$ represent the molar heat capacities of the as-prepared samples measured by the automatic adiabatic calorimeter and the corresponding result calculated from the eq 1, respectively.

For the spindle-shaped β-FeOOH:

$$C_{p,m}/\text{J} \cdot \text{K}^{-1} \cdot \text{mol}^{-1} = 61.32 + 39.19X - 11.78X^2 + 2.16X^3 + 0.57386X^4 \quad (3)$$

where $T_1 = 78.23$ K and $T_2 = 390.42$ K. The coefficient of determination of the fitting is $R^2 = 0.9999$, and the fitness standard error is $\delta = 0.211\ \text{J} \cdot \text{K}^{-1} \cdot \text{mol}^{-1}$.

The experimental molar heat capacities of the as-prepared rod- and spindle-shaped β-FeOOH are shown in Figure 4. It can be clearly seen that the molar heat capacities of the rod- and spindle-shaped particles are different over the temperature range of (78 to 390) K. The molar heat capacities of rod-like β-FeOOH is less than the spindle shape when the experimental temperature is less than about 175 K, but when the temperature is greater than 175 K, the molar heat capacities of the spindle-shaped β-FeOOH is less than that of the rod-like β-FeOOH.

The smoothed molar heat capacities of the β-FeOOH particles were calculated on the basis of the fitted eqs 1 and 3, and the results are listed in Table 2. The changes in the thermodynamic

Table 2. Smoothed Heat Capacities and Thermodynamic Functions of the As-Prepared β-FeOOH Particles[a]

T / K	$C_{p,m}$[b] / $J \cdot K^{-1} \cdot mol^{-1}$	ΔH[b] / $J \cdot mol^{-1}$	ΔS[b] / $J \cdot K^{-1} \cdot mol^{-}$	$C_{p,m}$[c] / $J \cdot K^{-1} \cdot mol^{-1}$	ΔH[c] / $J \cdot mol^{-1}$	ΔS[c] / $J \cdot K^{-1} \cdot mol^{-1}$
80	8.027	−10.101	−50.395	9.517	−10.203	−51.692
85	10.092	−10.056	−49.837	11.636	−10.150	−51.039
90	12.134	−10.001	−49.208	13.724	−10.087	−50.319
95	14.152	−9.935	−48.515	15.782	−10.013	−49.536
100	16.147	−9.859	−47.760	17.809	−9.929	−48.694
105	18.119	−9.773	−46.950	19.806	−9.835	−47.799
110	20.067	−9.678	−46.089	21.772	−9.731	−46.856
115	21.992	−9.573	−45.180	23.708	−9.618	−45.867
120	23.894	−9.458	−44.227	25.614	−9.494	−44.838
125	25.773	−9.334	−43.235	27.490	−9.361	−43.772
130	27.629	−9.200	−42.206	29.335	−9.219	−42.672
135	29.463	−9.058	−41.145	31.151	−9.068	−41.543
140	31.274	−8.906	−40.053	32.937	−8.908	−40.386
145	33.063	−8.745	−38.934	34.693	−8.739	−39.206
150	34.830	−8.575	−37.791	36.420	−8.561	−38.004
155	36.575	−8.397	−36.626	38.117	−8.375	−36.783
160	38.298	−8.209	−35.441	39.786	−8.180	−35.546
165	39.999	−8.014	−34.239	41.425	−7.977	−34.294
170	41.679	−7.810	−33.021	43.036	−7.766	−33.031
175	43.338	−7.597	−31.789	44.618	−7.546	−31.757
180	44.976	−7.376	−30.546	46.172	−7.320	−30.474
185	46.593	−7.147	−29.292	47.699	−7.085	−29.185
190	48.190	−6.910	−28.029	49.197	−6.843	−27.890
195	49.767	−6.665	−26.759	50.668	−6.593	−26.591
200	51.323	−6.413	−25.481	52.112	−6.336	−25.288
205	52.860	−6.152	−24.199	53.529	−6.072	−23.984
210	54.378	−5.884	−22.912	54.920	−5.801	−22.678
215	55.876	−5.608	−21.621	56.285	−5.523	−21.372
220	57.356	−5.325	−20.327	57.624	−5.238	−20.066
225	58.816	−5.035	−19.030	58.938	−4.946	−18.762
230	60.259	−4.737	−17.732	60.226	−4.649	−17.459
235	61.684	−4.432	−16.433	61.491	−4.344	−16.158
240	63.091	−4.120	−15.132	62.731	−4.034	−14.860
245	64.481	−3.801	−13.831	63.947	−3.717	−13.564
250	65.854	−3.476	−12.529	65.140	−3.394	−12.272
255	67.211	−3.143	−11.227	66.311	−3.066	−10.982
260	68.551	−2.804	−9.925	67.459	−2.731	−9.696
265	69.875	−2.457	−8.624	68.585	−2.391	−8.414
270	71.184	−2.105	−7.322	69.690	−2.045	−7.135
275	72.478	−1.746	−6.021	70.774	−1.694	−5.859
280	73.757	−1.380	−4.720	71.838	−1.338	−4.587
285	75.022	−1.008	−3.419	72.883	−0.976	−3.319
290	76.273	−0.630	−2.119	73.908	−0.609	−2.054
295	77.511	−0.245	−0.819	74.915	−0.237	−0.793
300	78.736	0.145	0.481	75.904	0.140	0.465
305	79.948	0.542	1.781	76.875	0.522	1.719
310	81.148	0.945	3.080	77.830	0.909	2.969
315	82.336	1.353	4.378	78.768	1.300	4.217
320	83.514	1.768	5.676	79.692	1.697	5.460
325	84.680	2.189	6.974	80.600	2.097	6.700
330	85.836	2.615	8.270	81.494	2.503	7.936
335	86.983	3.047	9.566	82.375	2.912	9.168
340	88.120	3.485	10.860	83.244	3.326	10.396
345	89.249	3.928	12.153	84.100	3.745	11.619
350	90.369	4.377	13.444	84.945	4.167	12.837
355	91.482	4.832	14.732	85.780	4.594	14.051
360	92.587	5.292	16.018	86.605	5.025	15.258
365	93.686	5.758	17.300	87.421	5.460	16.459
370	94.779	6.229	18.577	88.229	5.899	17.653
375	95.866	6.705	19.850	89.030	6.343	18.839
380	96.948	7.187	21.116	89.824	6.790	20.016
385	98.026	7.675	22.376	90.612	7.241	21.184
390	99.101	8.168	23.627	91.396	7.696	22.341
298.15	78.284	0	0	75.540	0	0

[a] $\Delta H = H(T/K) - H(298.15)$. $\Delta S = S(T/K) - S(298.15)$. [b] Rod-like β-FeOOH. [c] Spindle-shaped β-FeOOH.

functions of β-FeOOH, such as ΔH and ΔS, were also calculated by the following thermodynamic equations.

$$\Delta H = H(T/\mathrm{K}) - H(298.15) = \int_{298.15}^{T} C_{p,m} \mathrm{d}T \qquad (4)$$

$$\Delta S = S(T/\mathrm{K}) - S(298.15) = \int_{298.15}^{T} \frac{C_{p,m}}{T} \mathrm{d}T \qquad (5)$$

The calculated changes in the thermodynamic functions of β-FeOOH, such as ΔH and ΔS, relative to standard to the reference temperature 298.15 K, are given in Table 2 at 5 K intervals.

Conclusions

In summary, rod- and spindle-shaped β-FeOOH crystals were synthesized via a hydrothermal reaction. There are two mass loss steps over the temperature ranges, (25 to 200 and 200 to 520) °C. The molar heat capacities of the as-prepared β-FeOOH crystals were determined for the first time by a high-precision automatic adiabatic calorimeter over the temperature range of (78 to 390) K. The molar heat capacities of rod-like β-FeOOH are less than those of spindle-shaped β-FeOOH when the experimental temperature is less than about 175 K, but when the temperature is greater than 175 K, the molar heat capacities of spindle-shaped β-FeOOH are less than those of rod-like β-FeOOH. The function of the molar heat capacity with respect to thermodynamic temperature was established for the rod- and spindle-shaped β-FeOOH. The thermodynamic functions were derived on the basis of an established function and the relationships of thermodynamic functions.

Literature Cited

(1) Xiong, Y. J.; Xie, Y.; Chen, S. W.; Li, Z. Q. Fabrication of Self-Supported Patterns of Aligned β-FeOOH Nanowires by a Low-Temperature Solution Reaction. *Chem.—Eur. J.* **2003**, *9*, 4991–4996.

(2) Wang, X.; Chen, X. Y.; Gao, L. S.; Zheng, H. G.; Ji, M. R.; Tang, C. M.; Shen, T.; Zhang, Z. D. Synthesis of β-FeOOH and α-Fe_2O_3 nanorods and electrochemical properties of β-FeOOH. *J. Mater. Chem.* **2004**, *14*, 905–907.

(3) Shao, H. F.; Qian, X. F.; Yin, J.; Zhu, Z. K. Controlled morphology synthesis of β-FeOOH and the phase transition to Fe_2O_3. *J. Solid State Chem.* **2005**, *178*, 3130–3136.

(4) Wu, P. C.; Wang, W. S.; Huang, Y. T.; Sheu, H. S.; Lo, Y. W.; Tsai, T. L.; Shieh, D. B.; Yeh, C. S. Porous Iron Oxide Based Nanorods Developed as Delivery Nanocapsules. *Chem.—Eur. J.* **2007**, *13*, 3878–3885.

(5) Wang, Y.; Cao, J. L.; Wang, S. R.; Guo, X. Z.; Zhang, J.; Xia, H. J.; Zhang, S. M.; Wu, S. H. Facile Synthesis of Porous α-Fe_2O_3 Nanorods and Their Application in Ethanol Sensors. *J. Phys. Chem. C* **2008**, *112*, 17804–17808.

(6) Nitin, K.; Chaudhari., Y. J. S. Size Control Synthesis of Uniform β-FeOOH to High Coercive Field Porous Magnetic α-Fe_2O_3 Nanorods. *J. Phys. Chem. C* **2008**, *112*, 19957–19962.

(7) Flynn, C. M., Jr. Hydrolysis of Inorganic Iron (III) Salts. *Chem. Rev.* **1984**, *84*, 31–41.

(8) Sugimoto, T.; Muramatsu, A. Formation Mechanism of Monodispersed α-Fe_2O_3 Particles in Dilute $FeCl_3$ Solutions. *J. Colloid Interface Sci.* **1996**, *184*, 626–638.

(9) Mazeina, L.; Deore, S.; Navrotsky, A. Energetics of Bulk and Nano-Akaganeite, β-FeOOH: Enthalpy of Formation, Surface Enthalpy, and Enthalpy of Water Adsorption. *Chem. Mater.* **2006**, *18*, 1830–1838.

(10) Wu, P. C.; Wang, W. S.; Huang, Y. T.; Sheu, H. S.; Lo, Y. W.; Tsai, T. L.; Shieh, D. B.; Yeh, C. S. Porous Iron Oxide Based Nanorods Developed as Delivery Nanocapsules. *Chem.—Eur. J.* **2007**, *13*, 3878–3885.

(11) Tan, Z. C.; Sun, L. X.; Meng, S. H.; Li, L.; Zhang, J. B. Heat capacities and thermodynamic functions of p-chlorobenzoic acid. *J. Chem. Thermodyn.* **2002**, *34*, 1417–1429.

(12) Nan, Z.; Wei, C.; Yang, Q.; Tan, Z. C. Thermodynamic Properties of Carbon Nanotubes. *J. Chem. Eng. Data* **2009**, *54*, 1367–1370.

(13) Tan, Z. C.; Sun, G. Y.; Sun, Y.; Yin, A. X.; Wang, W. B.; Ye, J. C.; Zhou, L. X. An adiabatic low-temperature calorimeter for heat capacity measurement of small samples. *J. Therm. Anal.* **1995**, *45*, 59–67.

(14) Ditmars, D. A.; Ishihara, S.; Chang, S. S.; Bernstein, G.; West, E. D. Enthalpy and heat-capacity standard reference material: synthetic sapphire (α-Al2O3) from 10 to 2250 K. *J. Res. Natl. Bur. Stand.* **1982**, *87*, 159–163.

Received for review April 22, 2009. Accepted August 30, 2009. The financial support from the National Science Foundation of China (20753002) and the Natural & Scientific Grant of Jiangsu Province (BK2009181), China, is gratefully acknowledged.

JE900373Z